

Organizational Innovation of Apical Actin Filaments Drives Rapid Pollen Tube Growth and Turning

Xiaolu Qu^{1,5}, Ruihui Zhang^{1,5}, Meng Zhang^{1,2,5}, Min Diao^{1,2}, Yongbiao Xue^{3,4} and Shanjin Huang^{1,2,*}

¹Center for Plant Biology, School of Life Sciences, Tsinghua University, Beijing 100084, China

²Key Laboratory of Plant Molecular Physiology, Institute of Botany, Chinese Academy of Sciences, Beijing 100093, China

³State Key Laboratory of Molecular Developmental Biology, Institute of Genetics and Developmental Biology, Chinese Academy of Sciences, Beijing 100101, China

⁴Beijing Institute of Genomics, Chinese Academy of Sciences, Beijing 100101, China

⁵These authors contributed equally to this article.

*Correspondence: Shanjin Huang (sjhuang@tsinghua.edu.cn)

<http://dx.doi.org/10.1016/j.molp.2017.05.002>

ABSTRACT

Polarized tip growth is a fundamental cellular process in many eukaryotes. In this study, we examined the dynamic restructuring of the actin cytoskeleton and its relationship to vesicle transport during pollen tip growth in *Arabidopsis*. We found that actin filaments originating from the apical membrane form a specialized structure consisting of longitudinally aligned actin bundles at the cortex and inner cytoplasmic filaments with a distinct distribution. Using actin-based pharmacological treatments and genetic mutants in combination with FRAP (fluorescence recovery after photobleaching) technology to visualize the transport of vesicles within the growth domain of pollen tubes, we demonstrated that cortical actin filaments facilitate tip-ward vesicle transport. We also discovered that the inner apical actin filaments prevent backward movement of vesicles, thus ensuring that sufficient vesicles accumulate at the pollen tube tip to support the rapid growth of the pollen tube. The combinatorial effect of cortical and internal apical actin filaments perfectly explains the generation of the inverted “V” cone-shaped vesicle distribution pattern at the pollen tube tip. When pollen tubes turn, apical actin filaments at the facing side undergo depolymerization and repolymerization to reorient the apical actin structure toward the new growth direction. This actin restructuring precedes vesicle accumulation and changes in tube morphology. Thus, our study provides new insights into the functional relationship between actin dynamics and vesicle transport during rapid and directional pollen tube growth.

Key words: pollen tube, clear zone, apical actin structure, actin dynamics, vesicle trafficking, myosin

Qu X., Zhang R., Zhang M., Diao M., Xue Y., and Huang S. (2017). Organizational Innovation of Apical Actin Filaments Drives Rapid Pollen Tube Growth and Turning. *Mol. Plant.* **10**, 930–947.

INTRODUCTION

Tip growth is an extreme form of polarized cell growth that occurs exclusively from a single site (Franklin-Tong, 1999; Hepler et al., 2001; Cole and Fowler, 2006; Yang, 2008; Qin and Yang, 2011; Guan et al., 2013; Rounds and Bezanilla, 2013). It is important for morphogenetic and developmental processes in different eukaryotic organisms, including sexual reproduction in higher plants, nervous system development in mammals, and development and pathogenesis in fungi. To achieve this type of growth, tip-growing cells must direct the transport of vesicles to the apical region to maintain a distinct apical growth domain. Revealing how tip-growing cells generate and maintain this

domain is central to understanding the cellular mechanism of tip growth.

Pollen tubes in particular exhibit a prominent apical zone that is full of vesicles (Lancelle and Hepler, 1992). In living pollen tubes from many different species, the transport vesicles assume a distribution pattern with an inverted “V” cone shape (de Graaf et al., 2005; Lee et al., 2008; Kroeger et al., 2009; Zhang et al., 2010b; Qu et al., 2013; Stephan et al., 2014; Chang and Huang,

The Apical Actin Structure in Pollen Tubes

2015; Li et al., 2017). The vesicles carry materials necessary for membrane expansion and cell-wall synthesis and consequently are vital for pollen tube growth. Under the light microscope, the apical zone exhibits a more uniform texture than the rest of the cell body and has been defined as the “clear zone” (Lovy-Wheeler et al., 2007; Hepler and Winship, 2015). The presence of the clear zone has been described as an indicator of healthy and vigorous pollen tubes (Lovy-Wheeler et al., 2007). However, it remains an open question how the clear zone is generated and maintained during directional pollen tube growth (Hepler and Winship, 2015).

Underlying the generation of the clear zone, or in other words the unique zonation of the cytoplasm (Cheung and Wu, 2007), is the distinct organization of the actin cytoskeleton within different regions of the pollen tube (Ren and Xiang, 2007; Cheung and Wu, 2008; Chen et al., 2009; Staiger et al., 2010; Fu, 2015; Qu et al., 2015). Within the shank region, actin filaments are mainly arrayed into actin cables that are aligned with the long axis of the pollen tube (Cheung et al., 2008). Those longitudinally aligned actin cables are excluded from the tip of growing pollen tubes that are demonstrated to mediate cytoplasmic streaming (Gu et al., 2005; Ye et al., 2009; Wu et al., 2010). Within the subapical region, a prominent actin structure that is made up of short actin bundles is consistently captured but exhibits different appearances within pollen tubes from different species. Different names have therefore been given to them, such as actin fringe (Lovy-Wheeler et al., 2005; Dong et al., 2012), actin ring or collar (Kost et al., 1998; Gibbon et al., 1999; Fu et al., 2001), actin mesh (Geitmann et al., 2000; Chen et al., 2002), and actin funnel or basket (Vidali et al., 2001; Hormanseder et al., 2005). The difference in the morphology of the reported subapical actin structures could be due to different labeling approaches, since apical actin filaments turn over very quickly (Gibbon et al., 1999; Fu et al., 2001; Vidali et al., 2001) and are hard to preserve and visualize. It is possible that the reported morphological differences could be, to some extent, due to a true variation in the overall organization of actin filaments in different species. Certainly, it is also possible that those reported subapical actin structures represent a continuum of related structures each existing part of the time during pollen tube growth as proposed by Cheung et al. (2008). For this reason, Cheung et al. argued that it might be conceptually too confining to apply any single morphological descriptive to describe the subapical actin structure in growing pollen tubes and proposed the name “subapical actin structure” to describe actin structures at the subapex of pollen tubes (Cheung et al., 2008). In addition to the subapical F-actin, Yang’s group provided evidence showing the presence of a dynamic form of tip-localized F-actin in living tobacco pollen tubes, which is regulated by ROP signaling via two counteracting downstream pathways in pollen tubes (Fu et al., 2001; Gu et al., 2005). Nonetheless, actin filaments at the subapex and apex are extremely relevant to generation of the clear zone (Kroeger et al., 2009; Cheung et al., 2010; Hepler and Winship, 2015), since they are closely associated with each other in space (Lovy-Wheeler et al., 2005). In particular, a previous study in *Arabidopsis* showed that membrane-localized FH5 (formin homology5) mediates assembly of the subapical actin structure to facilitate vesicular trafficking within the apical dome (Cheung et al., 2010). In addition, a study by Yang’s group suggested

that ROP1-dependent apical actin promotes vesicle accumulation in the apex (Lee et al., 2008). However, how exactly actin filaments regulate transport and accumulation of vesicles remains to be explored. In this regard, careful documentation of the exact organization and dynamics of actin filaments within the growth domain during tube elongation, and comparison of pollen tubes from different species, may provide clues to help us answer this question.

There has been considerable debate about how the actin cytoskeleton might be involved in vesicle trafficking within the growth domain of pollen tubes, and in particular there has been a long-term debate about whether exocytotic vesicles arrive at the very tip or subapically in the pollen tube. Several hypotheses have been proposed regarding the function of subapical actin structures in the regulation of vesicle trafficking in pollen tubes (Geitmann and Emons, 2000). One hypothesis argues that the cortical fringe acts as a track for myosin motors to allow the transport of vesicles to precise sites in the apex of the pollen tube (Lovy-Wheeler et al., 2005); the other hypothesis argues that the subapical actin structure acts as a filter to create the apical vesicular zone (Kost et al., 1998; Cheung et al., 2008). In addition, it was also found that the apical actin filaments border the vesicle zone, and the subapical actin fringe structure was therefore assumed to constrain the apical vesicle zone (Kroeger et al., 2009). To examine the validity of these hypotheses, it is necessary to combine simultaneous visualization of actin dynamics and vesicles during pollen tube growth with actin-based genetic manipulations and pharmacological treatments, which we have done here using FRAP (fluorescence recovery after photobleaching) technology to visualize the transport of vesicles within the growth domain of wild-type (WT) pollen tubes or pollen tubes with altered actin cytoskeleton.

Here, we provide a unified view of the overall morphology and dynamics of apical actin filaments within pollen tubes, and further show that the differential organization of apical actin filaments in space might have a distinct function in the regulation of vesicle trafficking. Our results suggest that the development and elaboration of apical actin structure may represent an evolutionarily conserved strategy to ensure the rapidity of pollen tube growth for pollination and fertilization in flowering plants. These findings substantially advance our understanding of the actin-based cell regulatory mechanism underlying rapid and polarized pollen tube growth.

RESULTS

A Population of Apical Actin Filaments Is Associated with and Required for Normal Pollen Tube Growth

To decipher the relationship between apical actin filaments and pollen tube growth in *Arabidopsis*, we used time-lapse spinning disk confocal microscopy of live pollen tubes in which actin filaments were labeled with Lifeact-eGFP. We found that a population of apical actin filaments is continuously generated from the apical membrane, and generation of these filaments is tightly linked with pollen tube growth (Figure 1A–1C). We also noticed that when WT pollen tube growth was spontaneously delayed in a naturally growing pollen tube, the apical actin structure disappeared (Figure 1D–1F). We extended this result

by showing that treatment with a low dose of latrunculin B (LatB), which specifically depolymerized apical actin filaments (Supplemental Figure 1A), caused pollen tube growth inhibition (Figure 1G–1I). In addition, we found that growth inhibition in a naturally growing pollen tube was accompanied by disorganization of apical actin filaments (Figure 1J–1L). These results provide good evidence that apical actin polymerization and organization are required for normal pollen tube growth. To describe the overall organization of apical actin filaments, we examined longitudinal and transverse sections of growing pollen tubes, and found that the filaments are relatively dense at the cortex but are relatively sparse in the inner region of the pollen tube (Figure 1M and 1N). Specifically, some apical actin filaments are aligned longitudinally at the cortex; other apical actin filaments, however, extend into the inner region of the cytoplasm (Figure 1M and 1N; Supplemental Movie 1). Further observations showed that apical actin filaments are mainly generated from the apical membrane (Supplemental Figure 2A; Qu et al., 2013; Zhang et al., 2016a). These filaments frequently undergo bundling events (Supplemental Figure 2B and 2C), and the bundling level of actin filaments at the cortex is comparatively high (Supplemental Figure 2D). Based on these observations, a simplified schematic model was drawn to describe the overall organization of apical actin filaments (Figure 1O). Thus, we provide strong evidence that generation of the properly organized apical actin filaments is tightly linked with pollen tube growth.

Apical Actin Filaments Regulate Tip-Directed Accumulation of Vesicles and Generation of the Clear Zone

We next investigated how apical actin filaments may regulate the accumulation of apical vesicles and generation of the clear zone. Initially, we found that *Arabidopsis* pollen tubes contain a smooth region corresponding to the clear zone, and this zone is maintained during pollen tube growth (Figure 2A). Formation of the clear zone occurs with and precedes tube regrowth (Figure 2B), and it starts to disappear after the cessation of pollen tube growth in naturally growing pollen tubes (Figure 2C). We found that this zone is indeed full of transport vesicles in *Arabidopsis* pollen tubes (Figure 2D), and apical accumulation of vesicles coincides with formation of the clear zone (Figure 2E). We then showed that apical actin filaments are tightly associated with the clear zone (Figure 2F), and a properly organized apical actin structure is required for formation of the clear zone (Figure 2G). Next, we showed that the highly concentrated vesicles at the tip are surrounded by apical actin filaments, and the region occupied by the vesicles gradually became narrower as the distance from the tip increases (Figure 2H and 2I; Supplemental Movie 2). This finding suggests that vesicles are spatially restricted by apical actin filaments.

The regulatory role of actin in apical vesicle accumulation was demonstrated by showing that 3 nM LatB treatment caused dissipation of the vesicles from the pollen tube tip (Figure 2J). Given that apical actin polymerization is assumed to be mainly controlled by formins (Cheung et al., 2010; Liu et al., 2015; Li et al., 2017), the importance of apical actin filaments in regulating apical vesicle accumulation was also examined by treatment with SMIFH2 (small molecular inhibitor of formin

homology two domains) (Rizvi et al., 2009). SMIFH2 treatment inhibited pollen tube growth and apical actin polymerization in a dose-dependent manner (Supplemental Figure 1B). We found that dissipation of vesicles from the pollen tube tip occurred concurrently with the SMIFH2-mediated inhibition of apical actin polymerization (Figure 2K). In line with this finding, *prf4 prf5* mutant pollen tubes, which are defective in apical actin polymerization and formation of apical actin structures (Figure 2L–2N; Liu et al., 2015), exhibited defects in the apical accumulation of vesicles (Figure 2O and 2P). In addition, we found that apical vesicle accumulation was impaired when apical actin filaments became disorganized in WT and *vin2 vin5* pollen tubes that periodically exhibit abnormal accumulation of apical actin filaments (Supplemental Figure 3; Qu et al., 2013). Taken together, these results demonstrate that a properly organized apical actin structure is required for apical vesicle accumulation in pollen tubes.

Apical Actin Filaments at the Cortex Drive Tip-Directed Vesicle Transport Presumably by Providing Molecular Tracks for Myosin Motors

To determine exactly how actin filaments regulate apical vesicle accumulation, we used time-lapse microscopy and found that reformation of a bright apical actin structure precedes apical vesicle accumulation in a WT pollen tube (Figure 3A and 3B). We confirmed this by showing that apical vesicle accumulation followed soon after recovery of the apical actin structure in LatB-treated pollen tubes (Figure 3C and 3D). Given that it was hypothesized that membrane-originated apical actin filaments are nucleated by formins, which are barbed end actin polymerases (Cheung et al., 2010; Qu et al., 2013), apical actin filaments may cooperate with barbed end-directed myosin XIs (Lee and Liu, 2004) to drive tip-ward vesicle movement. To test this notion, we treated pollen tubes with 2,3-butanedione monoxime (BDM), which was originally shown to antagonize the ATPase activity of myosin II and inhibit the activity of plant myosin *in vitro* (Tomimaga et al., 2000; Funaki et al., 2004) and the cytoplasmic streaming and organelle movement in living plant cells (Nebenfuhr et al., 1999; Holweg et al., 2003; Higaki et al., 2006). We found that BDM induced the dissipation of vesicles from the apical region of the tube (Figure 3E). This implicates that the activity of myosin is required for apical accumulation of vesicles.

Myosin motors selectively interact with actin tracks that have different degrees of bundling or are decorated with different actin bundling proteins (Nagy et al., 2008; Brawley and Rock, 2009). We therefore investigated tip-directed vesicle transport in *Arabidopsis* strains with altered filament binding status due to mutations in genes encoding actin-binding proteins. Indeed, we found that *fim5* mutant pollen tubes, which have disorganized apical actin filaments (Supplemental Figure 4A; Zhang et al., 2016a, 2016b), exhibited defects in apical vesicle accumulation (Supplemental Figure 4B and 4C). To determine whether cortical or internal or both types of apical actin filament are vital for tip-directed vesicle transport, we performed FRAP in pollen tubes expressing *Lat52::YFP-RabA4b*. We found that the fluorescence recovered first at the cortex within the tip region (Figure 3F; Supplemental Movie 3), suggesting that vesicles were transported to the tip along apical actin filaments at the cortex. Thus, the results showed that cortical apical actin

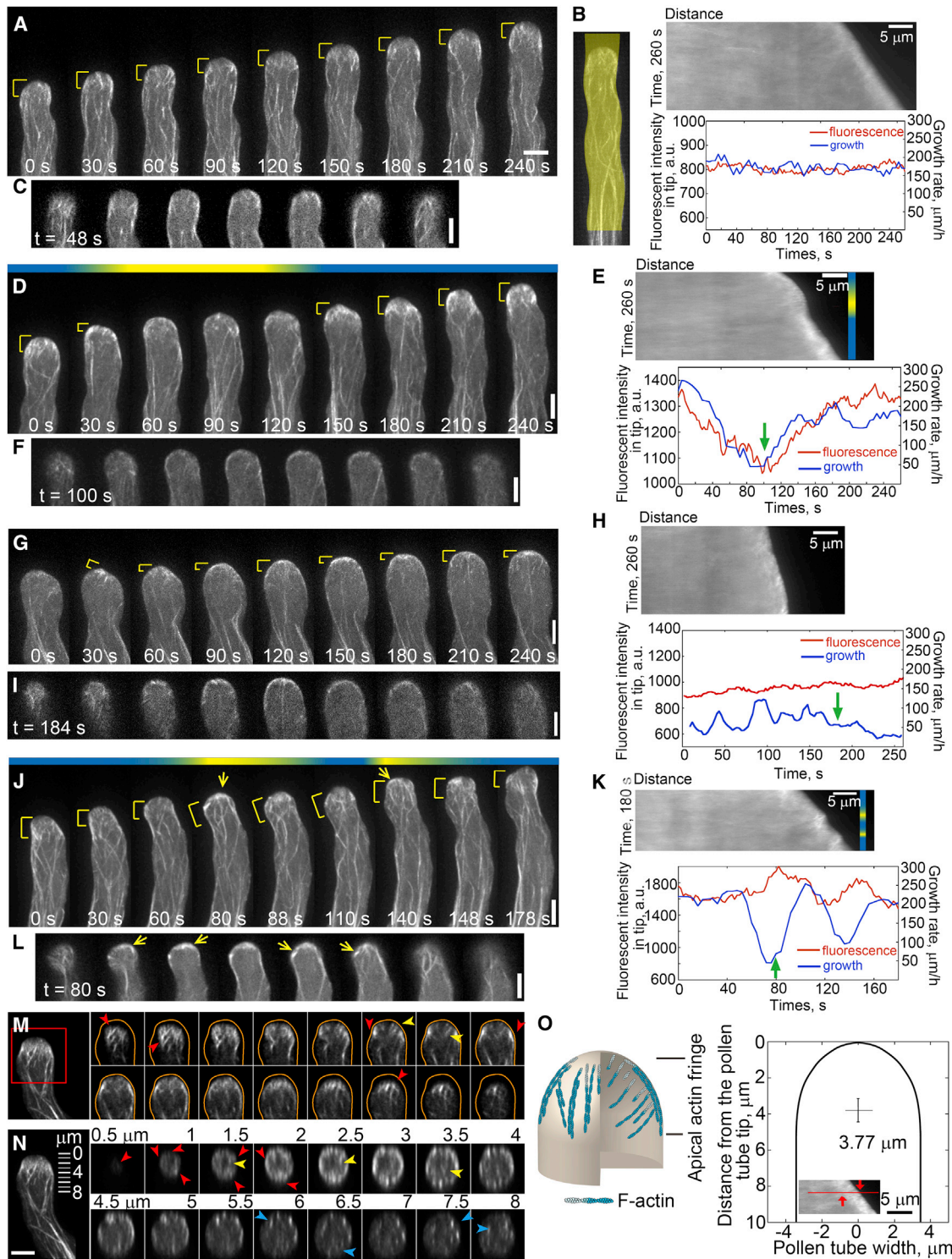


Figure 1. Apical Actin Filaments Are Associated with and Required for Pollen Tube Growth and Are Arranged into a Distinct Structure.

(A) Time-lapse images of actin filaments, labeled by Lifeact-eGFP, in a growing wild-type (WT) pollen tube.

(B) Kymograph analysis of images shown in (A). The left panel indicates the region covered by the kymograph analysis and the right panel shows a plot of the velocity of pollen tube growth and the amount of apical F-actin versus time.

(C) z series optical sections of the pollen tube at 48 s derived from the time-lapse analysis shown in (A).

(D) Time-lapse images of actin filaments in another growing WT pollen tube.

(E) Kymograph analysis of apical actin filaments during pollen tube growth. The colored band corresponds to that above the image in (D). Blue and yellow colored stages indicate periods of normal growth and delayed growth, respectively.

(legend continued on next page)

filaments drive tip-ward vesicle transport, presumably by providing tracks for myosin motors (Figure 3G).

Internal Apical Actin Filaments May Act as a Physical Barrier to Block the Backward Movement of Vesicles

Vesicles are transported along the cortex and released so that they accumulate at the extreme apical region centered at the polar axis. This implies that formation of an inverted “V” cone-shaped vesicle distribution pattern occurs during the backward movement of vesicles. In support of this, a previous study showed that uptake of FM4-64 results in a distinct staining pattern in the apical region, which corresponds spatially to the cone-shaped apical vesicle accumulation pattern (Parton et al., 2001). To further demonstrate this, we performed FRAP experiments on pollen tubes expressing *Lat52::YFP-RabA4b* with the tip kept unbleached. The results showed that vesicles indeed recovered in an inverted “V” cone-shaped distribution pattern (Figure 4A and 4B; Supplemental Movie 4). Given that vesicles are surrounded by apical actin filaments (Figure 2H; Supplemental Movie 2), it is very likely that the apical actin filaments may spatially restrict the vesicles. Considering that some apical actin filaments extend into the inner region of the cytoplasm, they might play an active role in regulating the backward movement of vesicles.

To understand how internal apical actin filaments regulate the backward movement of vesicles, we sought to model their distribution pattern. The theoretical shape of a pollen tube in the medial section was initially drawn (Figure 4C), and the location of each internal apical actin filament was determined from three parameters as described in Figure 4D. Based on the assumption that actin filaments originate equally from all parts of the apical membrane, and taking into account the two parameters in Figure 4C, the filament length distribution (Figure 4E), and the average filament angles (Figure 4F), we generated an initial overall apical filament distribution (Supplemental Figure 5A). Given that apical actin filaments have differential lifetimes at different locations (Supplemental Figure 5B), a refined model of apical actin filament distribution was generated after taking this into account (Figure 4G). The modeling result showed that actin filaments are relatively short and sparse at the tip, which might allow the released vesicles to accumulate there. In addition, the model allows us to speculate that internal apical actin filaments likely act as a

physical barrier to block the backward movement of vesicles, and consequently the vesicle-occupied region narrows down gradually from the tip to the base.

To test this hypothesis, we initially performed an FRAP experiment similar to the one described above except that we added 3 nM LatB to abolish the internal apical actin filaments (Figure 4H). The recovered vesicles became more diffuse in the apical region (Figure 4I). We extended this result by showing that, after inhibition of apical actin polymerization by treatment with SMIFH2 (Figure 4J), vesicles cannot recover to the regular inverted “V” cone-shaped distribution (Figure 4K; Supplemental Movie 5). A similar finding was obtained in *prf4 prf5* mutant pollen tubes (Figure 4L and 4M). In addition, we found that within *fim5* pollen tubes, which have disorganized internal apical actin filaments (Figure 4N), vesicles cannot recover their cone-shaped distribution (Figure 4O). These data demonstrate that the presence and proper organization of internal apical actin filaments are required for their role in regulating backward movement of vesicles. These internal filaments presumably act as a physical barrier to shape the apical vesicle distribution pattern (Figure 4P).

Apical Actin Filaments Prevent the Invasion of Large Organelles into the Pollen Tube Tip

To uncover how apical actin filaments prevent apical invasion of large organelles, we used YFP-ARA7 as the marker, because endosomes decorated with this fusion protein were previously shown to be excluded from the pollen tube tip (Zhang et al., 2010b). By tracking individual YFP-ARA7-positive endosomes, we found that these vesicles were excluded from the region occupied by apical actin filaments (Figure 5A). YFP-ARA7-positive endosomes moved toward the tip, but then reversed their direction of travel when they reached the base of the region occupied by apical actin filaments (Figure 5B and 5C). The requirement for apical actin filaments to prevent the invasion of large organelles was demonstrated by showing that 3 nM LatB treatment induced apical invasion of YFP-ARA7-decorated endosomes (Figure 5D). We extended this result by showing that inhibition of apical actin polymerization with SMIFH2 treatment caused gradual apical invasion of YFP-ARA7-decorated endosomes (Figure 5E). A similar finding was obtained in *prf4 prf5* mutant pollen tubes (Figure 5F and 5G). In addition, we found that YFP-ARA7-decorated endosomes invaded into the tip of *vln2 vln5* and *fim5*

(F) z series images of actin filaments at 100 s derived from the time-lapse series shown in (D) and indicated by the green arrow in (E).

(G) Time-series projection images of actin filaments in a pollen tube in the presence of 3 nM LatB.

(H) Kymograph analysis of apical actin filaments in the pollen tube shown in (G).

(I) z series images of actin filaments at 184 s derived from the time-lapse images shown in (G) and indicated by the green arrow in (H).

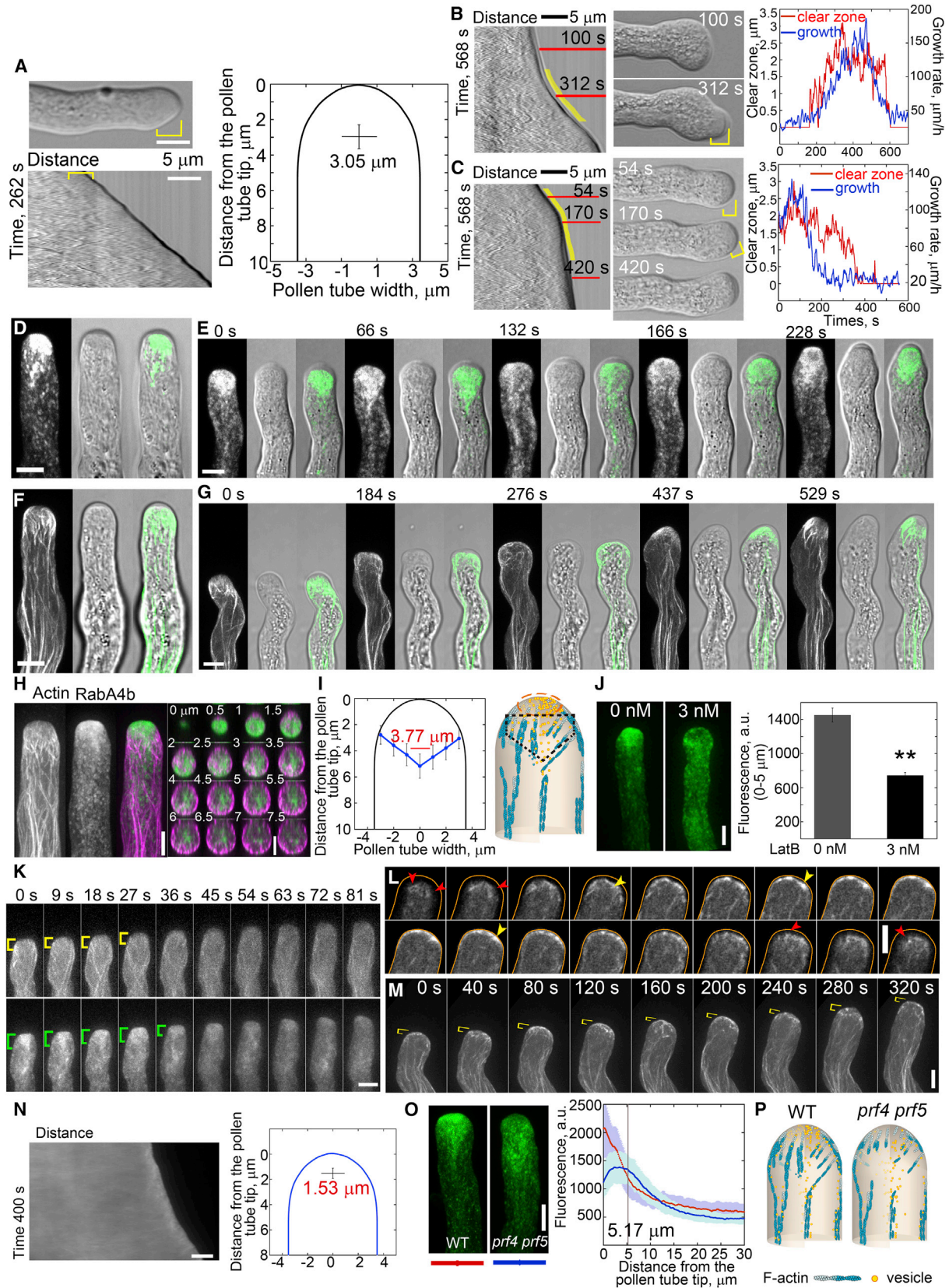
(J) Time-lapse image of actin filaments in a growing WT pollen tube.

(K) Kymograph analysis of actin filaments in the pollen tube shown in (J).

(L) z series images of apical actin filaments at 80 s derived from the time-series images shown in (J). The growth rate of the pollen tube at this time point is indicated by the green arrow in the plot in (K). Yellow brackets indicate bright apical actin filaments in (A), (D), (G), and (J). Yellow arrows indicate the accumulation of actin filaments at the extreme apex in (J) and (L). Bars, 5 μ m.

(M and N) Longitudinal sections (M) and transverse sections (N) of a WT pollen tube, showing the actin filaments. The left panels in (M) and (N) show the projection images. The orange lines indicate the edge of the pollen tube. The red and yellow arrowheads indicate actin filaments at the cortex and inner regions, respectively. The blue arrowheads indicate actin filaments in the shank region. See the three-dimensional Supplemental Movie 1 showing the spatial organization of apical actin filaments.

(O) Schematic organization of apical actin filaments in the pollen tube. The average length and distance of the actin fringe from the pollen tube tip was determined by kymograph analysis (inset image in the right panel the distance between red arrows represents the length of apical actin fringe). The average length (mean \pm SD) of the actin fringe is $3.77 \pm 0.65 \mu$ m, $n = 21$.



(legend on next page)

pollen tubes, which have disorganized apical actin filaments (Figure 5H–5K). This suggests that proper organization of apical actin filaments is also required for their role in excluding large organelles. We used statistical analysis to compare the distance from the tip of the pollen tube at which YFP-ARA7-decorated vesicles reversed their direction of travel in different strains. The distance is significantly reduced in *prf4 prf5*, *vln2 vln5*, and *fim5* pollen tubes compared with WT pollen tubes (Figure 5L). Taken together, these results provide good evidence that apical actin filaments prevent the apical invasion of large vesicles.

Reorientation of Apical Actin Structure Is an Early Event During the Turning of Pollen Tubes

To determine how apical actin filaments are involved in the turning of pollen tubes, we used time-lapse microscopy and found that during the turning process, the whole apical actin structure reorients, and this reorientation precedes changes in tube morphology (Figure 6A). During the reorientation of the apical actin structure toward the new tube growth direction, apical actin filaments on the side of the tip facing the new growth direction underwent a process of initial depolymerization and subsequent repolymerization (Figure 6A and 6B). Specifically, after elimination of the old apical actin filaments, new actin filaments were generated from the apical membrane and then underwent bundling to form actin bundles at the cortex (Figure 6C and 6D). However, actin filaments on the opposite side of the turning pollen tube underwent an increase in the extent of bundling (Figure 6E and 6F). This could be due to an upregulation of actin polymerization, or

an increase in filament bundling, or both. We next found that reorientation of the apical actin structure preceded the accumulation of apical vesicles in the region of the tip closest to the new growth direction (Figure 6G–6J; Supplemental Movie 6). This demonstrates that the apical actin structure reorients to direct vesicle transport toward the new growth direction to finally allow successful tube turning.

DISCUSSION

Our understanding of how actins perform their functions during pollen tube growth and turning has been hindered by the fact that we still lack a unified view regarding the overall organization and dynamics of actin filaments within the pollen tube growing domain. Here, we demonstrate that apical actin filaments are organized into a structure that is distinct from the shank-oriented longitudinal actin cables. The spatial distribution of apical actin filaments is well suited to the function of tip-directed vesicle trafficking that supports rapid pollen tube growth. This study greatly enhances our knowledge of the mechanism of action of actin in regulating polarized pollen tube growth and provides a significant advance toward understanding the cellular basis of rapid polarized pollen tube growth.

Shank-Oriented Longitudinal Actin Cables and Apical Actin Structure Represent Two Major Actin Structures in Pollen Tubes

It is generally accepted that actin filaments are packed into actin cables that align to the long axis of the pollen tube within the

Figure 2. The Apical Actin Structure Is Required for Apical Vesicle Accumulation and Generation of the Clear Zone in Pollen Tubes.

(A) Visualization and quantification of a smooth region corresponding to the clear zone in *Arabidopsis* pollen tubes. The yellow brackets indicate the clear zone. The average distance of the base of the clear zone from the tip was calculated as $3.05 \pm 0.69 \mu\text{m}$ (mean \pm SD) based on measurements from kymograph analysis (lower left panel) of 15 pollen tubes.

(B and C) Visualization and quantification of the clear zone during tube regrowth **(B)** and growth inhibition **(C)** in naturally growing pollen tubes. Yellow lines in the left panels indicate the regrowth and growth inhibition stage, respectively. Red lines in the left panels show the times at which the pollen tube images in the middle panels were taken: 100 s and 312 s in **(B)** and 54 s, 170 s, and 420 s in **(C)**. The right panels show plots of the distance of the base of the clear zone from the tip and the pollen tube growth rate versus time. Yellow brackets in the middle panels indicate the clear zone.

(D) Dual visualization of the clear zone and RabA4b-positive transport vesicles.

(E) Time-lapse images of dual visualization of vesicles and the clear zone in a pollen tube.

(F) Dual visualization of actin filaments and the clear zone in a pollen tube.

(G) Time-lapse images of dual visualization of actin filaments and the clear zone in a pollen tube.

Images at different time points from left to right in **(E)** and **(G)** show naturally growing pollen tubes at the stages of normal growth, growth reduction, growth inhibition, regrowth, and normal growth, respectively.

(H) Dual visualization of actin filaments and RabA4b-positive vesicles in a pollen tube. Actin and vesicles are pseudocolored magenta and green, respectively. The right panel shows transverse sections of the merged image. See the three-dimensional Supplemental Movie 2 showing the spatial relationship between actin filaments and RabA4b-positive vesicles.

(I) Statistics and schematic model of apical vesicle distribution and its association with actin filaments. The number ($3.77 \mu\text{m}$) shown in the left panel is the average length of the apical actin structure measured early in Figure 1O. The orange region contains dense small vesicles but fewer actin filaments; the region enclosed within the black dashed line indicates the tail region of the inverted “V” cone, which contains vesicles that are surrounded by apical actin filaments.

(J) Visualization and quantification of vesicles in the absence and presence of 3 nM LatB. The values represent mean \pm SE, $n = 50$, $**P < 0.01$ by Student’s *t*-test.

(K) Simultaneous visualization of actin filaments and vesicles in the presence of 100 μM SMIFH2. Yellow and green brackets indicate apical actin filaments and vesicles, respectively.

(L) z series images of actin filaments in a *prf4 prf5* pollen tube. Red arrowheads and yellow arrowheads indicate actin filaments at the cortex and inner region, respectively.

(M) Time-lapse images of actin filaments in a *prf4 prf5* pollen tube. Yellow brackets indicate apical actin filaments.

(N) Kymograph analysis of apical actin filaments in a *prf4 prf5* pollen tube. The average distance of the base of the apical actin structure from the tip was measured and is indicated in the image.

(O) Visualization and quantification of vesicles in WT and *prf4 prf5* pollen tubes. The left panel shows images of the vesicles, and the right panel shows quantification of the relative amount of vesicles, based on measuring the fluorescence at different distances from the tip. Red line, WT; blue line, *prf4 prf5*.

(P) Simple schematic distribution of apical actin filaments and vesicles in WT and *prf4 prf5* pollen tubes.

Bars, 5 μm in all images.

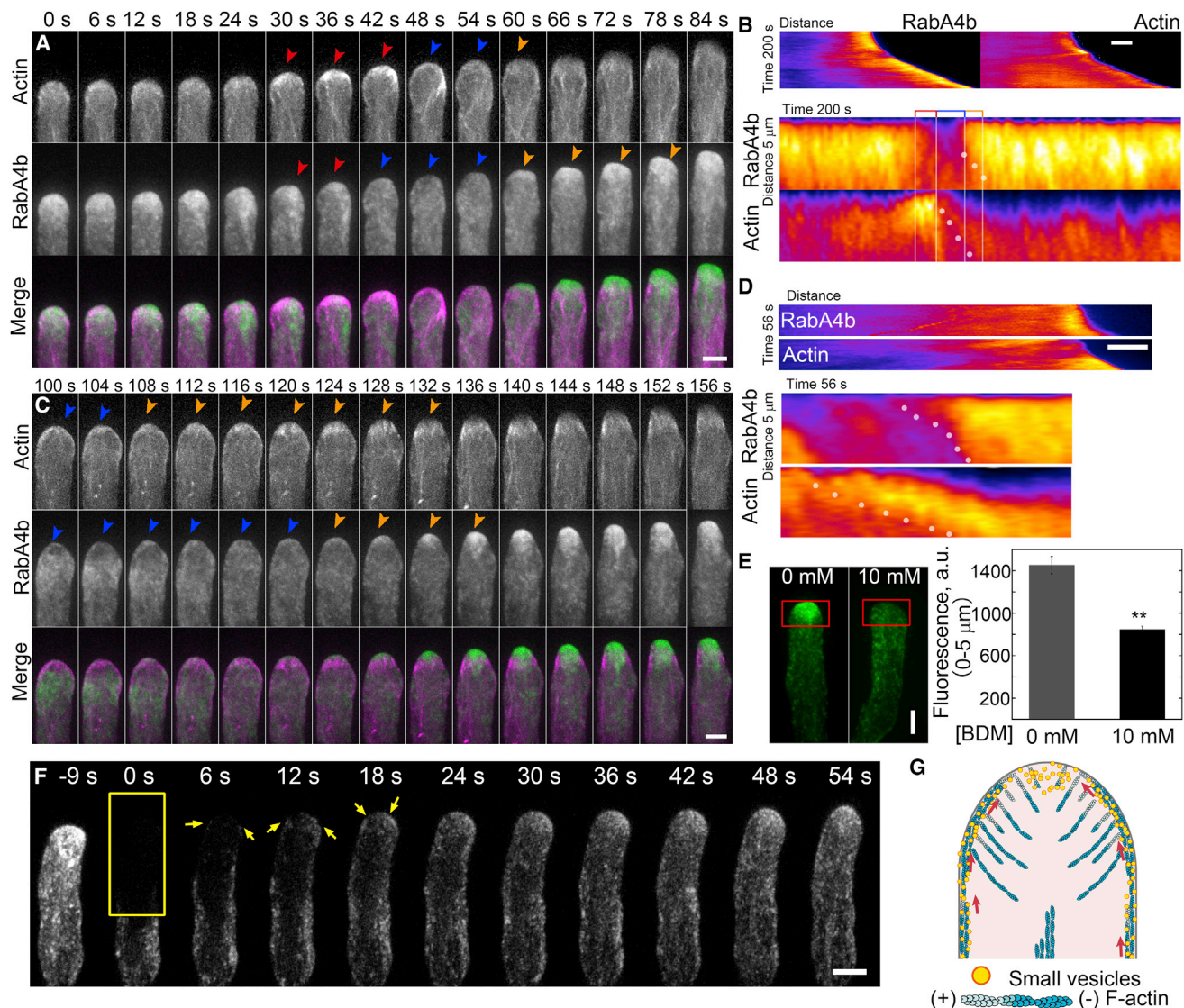


Figure 3. Apical Actin Filaments at the Cortex Drive Tip-directed Transport of Vesicles, Presumably by Providing Molecular Tracks for Myosin Motors.

(A and C) Time-lapse images of dual visualization of actin filaments and RabA4b-positive vesicles in the absence of LatB (A) or after treatment with LatB (3 nM) (C) in pollen tubes. Red, blue, and orange arrowheads indicate the accumulation, disappearance, and recovery, respectively, of apical actin filaments and YFP-RabA4b.

(B and D) Kymograph analysis of both actin filaments and vesicles in the images shown in (A) and (C), respectively. Warm and cold colors indicate high and low fluorescence intensity, respectively. The lower panel shows enlarged kymograph images of the pollen tube tip in the top panels. The red box indicates the period in which no obvious apical vesicle accumulation occurred while actin filaments accumulated. The blue box indicates the period of actin filament repolymerization, which was followed by apical vesicle accumulation. The yellow box indicates the period during which vesicles start to accumulate. White dots indicate the elongating ends of actin filaments and the edge of the region of vesicle accumulation.

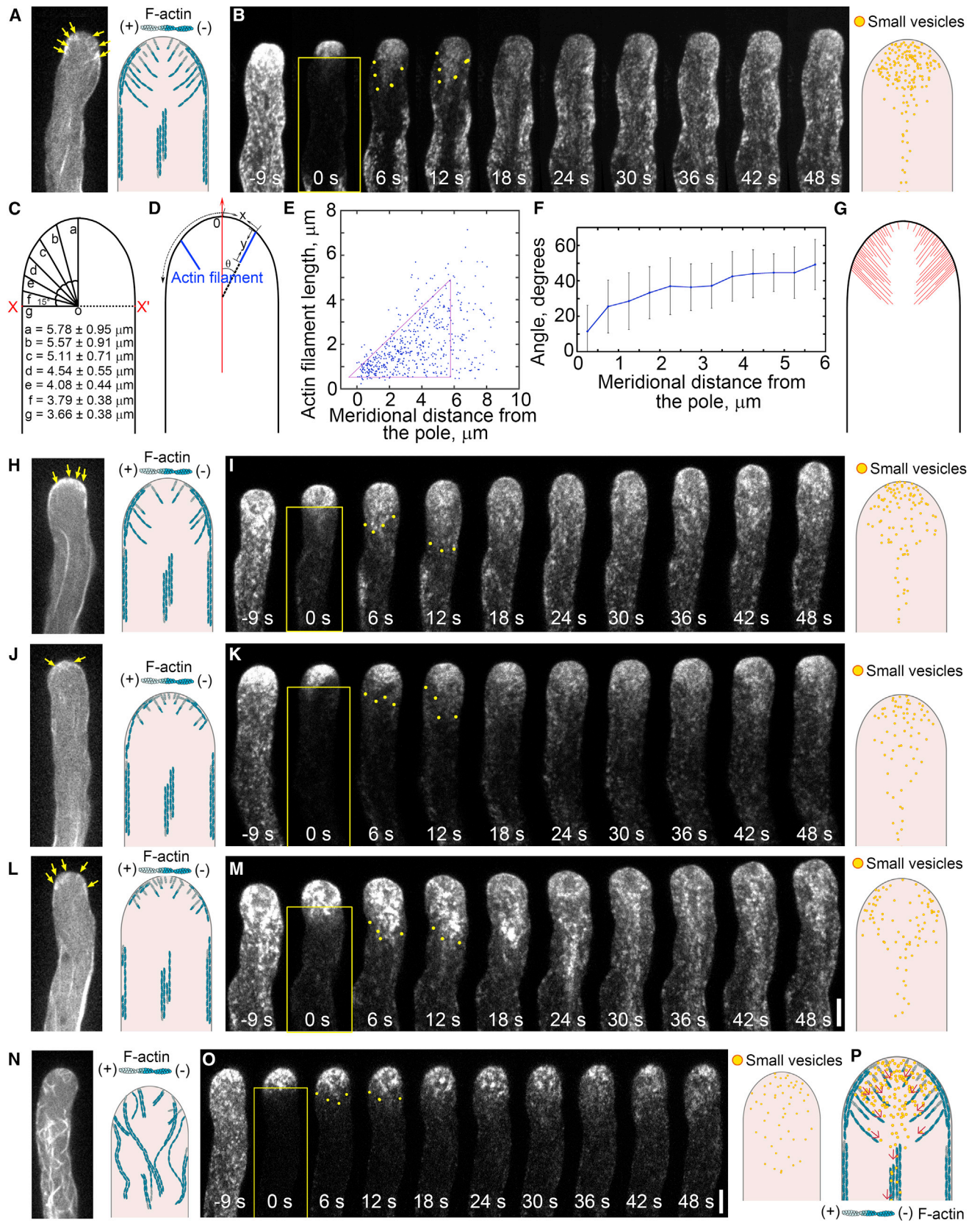
(E) Visualization and quantification of RabA4b-positive vesicles in the pollen tube in the absence or presence of 10 mM BDM. Red boxes indicate the regions for quantification. The right panel shows quantification of the relative amount of vesicles, based on fluorescence intensity measurement from 50 pollen tubes. Values represent mean ± SE, ***P* < 0.01 by Student's *t*-test.

(F) Time-lapse images of RabA4b-positive vesicles before and after photobleaching in the pollen tube. The yellow box indicates the photobleached region. Yellow arrows indicate the recovery sites of vesicles. See Supplemental Movie 3 for the entire series.

(G) Schematic model of tip-directed vesicle transport along apical actin filaments at the cortex. Red arrows indicate the direction of vesicle transport. Bars, 5 μm in all images.

shank region to mediate cytoplasmic streaming. By comparison, the existing published data provide rather disparate reports of the organization of the F-actin cytoskeleton within the growth domain of the pollen tube. Nonetheless, previous observations of the actin cytoskeleton in both fixed and living pollen tubes

from a variety of species allow a consensus view to be reached that actin filaments are arrayed into at least three distinct structures (Kost et al., 1998; Gibbon et al., 1999; Geitmann et al., 2000; Fu et al., 2001; Lovy-Wheeler et al., 2005; Cheung et al., 2008; Vidali et al., 2009; Wu et al., 2010; Zhang et al., 2010a;



(legend on next page)

Dong et al., 2012; Su et al., 2012; Qu et al., 2013; Zhu et al., 2013; Qin et al., 2014; Zhou et al., 2015; Li et al., 2017). We found that apical actin filaments mainly originate from the apical membrane and extend for about 4 μm into the cytoplasm to form a structure that is distinct from the shank-oriented longitudinal actin bundles in *Arabidopsis* pollen tubes (Figure 1). Given that these apical actin filaments are assumed to have the same origin, we think it is better to view them as a whole, and we have defined them here as the “apical actin structure.” Therefore, based on our observations, actin filaments are arranged into two major distinct structures in the pollen tube: the shank-oriented longitudinal actin cables and the apical actin structure. Importantly, we found that apical actin filaments are spatially distinct, some actin filaments are aligned longitudinally at the cortex (Figure 1M and 1N), and these correspond to the previously described actin fringe structure (Lovy-Wheeler et al., 2005; Vidali et al., 2009; Dong et al., 2012; Rounds et al., 2014). We believe that the apical actin structure revealed by decoration with Lifeact-eGFP in living pollen tubes represents the real situation, since decoration of actin filaments with the native FIM5-eGFP reveals a similar apical structure (Zhang et al., 2016a). Interestingly, we found that apical actin filaments are arranged into a similar structure and assume a similar spatial relationship with the clear zone in lily and tobacco pollen tubes (Supplemental Figure 6). This suggests that formation of a unique apical actin structure is a common design principle for all pollen tubes, regardless of species. Given that apical actin polymerization and subsequent organization positively correlate with pollen tube growth, an important question that remains to be answered in the future is how the generation and maintenance of the apical actin structure are

precisely regulated during rapid and directional pollen tube growth. It also remains to be addressed how the apical actin structure coordinates with the shank-oriented longitudinal actin cables to drive various intracellular trafficking events within the pollen tube.

Apical Actin Structure Is Well Suited to Tip-Directed Vesicle Transport and Accumulation for Supporting Sustainable Pollen Tube Growth and Turning

To support rapid and sustainable pollen tube growth, the materials necessary for cell-wall synthesis and membrane expansion need to be delivered to the expanding point of pollen tubes for the exocytosis. However, there has been a long-time debate in the pollen tube field regarding whether exocytic vesicles arrive to the very tip or subapically. Our FRAP analysis showed that tipward moving fluorescent vesicles reappear first within the tip region (Figure 3F), which suggests that exocytosis occurs at the extreme apex of the pollen tube. In line with this, we previously found that membrane-originated actin filaments at the extreme apex move laterally with the membrane flow during pollen tube growth (Qu et al., 2013). Our study is therefore consistent with the classical view that exocytosis occurs at the extreme apex of pollen tubes (Steer and Steer, 1989; Derksen et al., 1995). In support of this notion, it was shown that exocytosed protein markers, such as AtPRK1-GFP and NtPPME1-GFP, were incorporated into the membrane at the extreme tip of pollen tubes (Bosch et al., 2005; Lee et al., 2008; Wang et al., 2013; Luo et al., 2016). In further support of this notion, it was shown that the exocyst SEC3a subunit accumulates at or close to the tip plasma membrane that

Figure 4. Internal Apical Actin Filaments Shape Apical Vesicle Distribution Presumably by Acting as a Physical Barrier.

- (A) Actin filaments in a WT pollen tube.
 (B) Images of RabA4b-positive vesicles before and after photobleaching. See Supplemental Movie 4 for the entire series.
 (C) Description of the theoretical shape of the pollen tube. The middle longitudinal section of the pollen tube is presented. The junction points between the curved top and the cylindrical bottom of the pollen tube were defined as X and X', respectively, and the central point of the line connecting X to X' was defined as O. A line parallel to the growth axis starting from O was drawn and defined as line a, and the line connecting O to X was defined as line g. Lines b to f were drawn at 15-degree intervals starting from O. The lengths of the lines a to g were measured from pollen tube images collected by laser scanning confocal fluorescence microscopy, $n = 30$. Based on the average length of each line, the outer contour of the pollen tube was drawn.
 (D) Sketch of the measurement of the length and distribution angles of apical actin filaments in the inner region of pollen tubes. Single optical sections of actin filament images revealed by decoration with Lifeact-eGFP were used for the measurements. The extreme tip of the pollen tube was defined as point O, and a line (red) parallel to the growth axis of the pollen tube was drawn. Each actin filament was characterized by its length (y) and its distance from point O (x), as well as the angle formed between the actin filament and the red line (θ). Given that the shape of pollen tubes is determined as described in (C), the combination of parameters x , y , and θ can precisely position an actin filament. The curved dashed black arrow indicates the apical dome that is occupied by apical actin filaments.
 (E) Distribution of the length of actin filaments (colored blue in D). $n > 500$. The pink triangle indicates the region occupied by apical actin filaments.
 (F) Statistical analysis of the angles formed between apical actin filaments and the tube growth axis. $n > 500$, bars indicate SD.
 (G) Schematic diagram showing the distribution of apical actin filaments after correction for the variation in filament lifetime. The number of actin filaments within different regions was normalized based on the measurement of filament lifetime in Supplemental Figure 5B.
 (H) Actin filaments in the middle section in the presence of 3 nM LatB.
 (I) Time-series images of YFP-RabA4b before and after photobleaching in the presence of 3 nM LatB.
 (J) Actin filaments in the middle section in the presence of 100 μM SMIFH2.
 (K) Time-series images of YFP-RabA4b before and after photobleaching in the presence of 100 μM SMIFH2. See Supplemental Movie 5 for the entire series.
 (L) Actin filaments in a *prf4 prf5* pollen tube.
 (M) Time-series images of YFP-RabA4b before and after photobleaching in a *prf4 prf5* pollen tube. Bar, 5 μm in (M) for (A–H).
 (N) Actin filaments in a *fim5* pollen tube.
 (O) Time-series images of YFP-RabA4b before and after photobleaching in a *fim5* pollen tube. Bar, 5 μm in (O) for (N) and (O). The right panel in (B), (I), (K), (M), and (O) shows a model of the vesicle recovery pattern and the right panel in (A), (H), (J), (L), and (N) shows the simple schematic organization of actin filaments. In (B), (I), (K), (M), and (O), yellow boxes indicate the photobleached regions, and yellow dots indicate the edge of the shape formed by the backward movement of vesicles. Yellow arrows in (A), (H), (J), and (L) indicate apical actin filaments.
 (P) Schematic model of the backward movement of vesicles from the tip. Red arrows indicate the direction of vesicle movement after being blocked by the internal apical actin filaments.

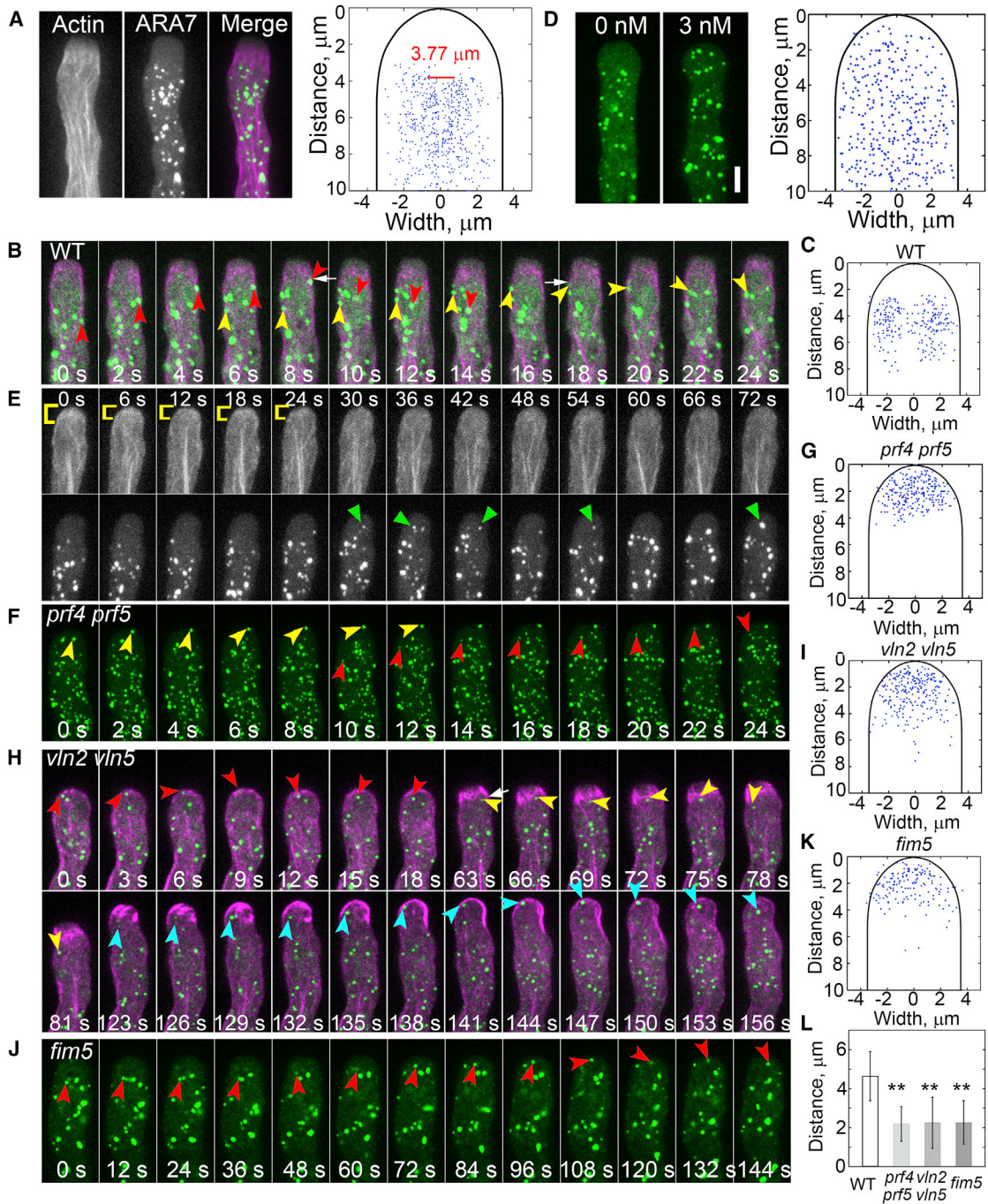


Figure 5. The Apical Actin Structure Prevents the Invasion of ARA7-Decorated Endosomes into the Tip.

(A) Visualization and quantification of actin filaments and ARA7-positive endosomes. The right panel shows quantification of the distance of the top edge of the region containing ARA7-positive endosomes from the tip. In total, 594 endosomes were measured in 17 pollen tubes.

(B) Time-lapse images of actin filaments and ARA7-positive endosomes in a WT pollen tube. Red and yellow arrowheads indicate the tracked vesicles, and white arrows indicates the point at which the movement of the vesicle reverses.

(C) Quantification of the position at which ARA7-positive endosomes reverse their direction of movement in a WT pollen tube. In total, 260 motile endosomes were tracked in 43 pollen tubes.

(D) The distribution of ARA7-positive endosomes in the presence and absence of 3 nM LatB. The right panel shows the distribution of ARA7-labeled endosomes, as in the right panel of (A). A total of 390 endosomes were measured in 21 pollen tubes.

(E) The effect of SMIFH2 treatment (100 μM) on actin filaments (upper panel) and ARA7-positive endosomes (lower panel). Yellow brackets indicate apical actin filaments, and green arrowheads indicate endosomes that invade into the tip.

(F) Time-series images of ARA7-positive endosomes in a *prf4 prf5* pollen tube. Yellow and red arrowheads indicate the tracked vesicles.

(legend continued on next page)

marks the direction of pollen tube elongation (Bloch et al., 2016). Our findings also support the classical view on the generation of the reverse fountain pattern of cytoplasmic streaming in angiosperm pollen tubes (de Win et al., 1999; Lovy-Wheeler et al., 2007; Bove et al., 2008; Ye et al., 2009; Wu et al., 2010). In this model, large organelles move tip-ward along the cortex and reverse their direction at the subapical region, before moving backward in the middle region of the pollen tube. Apical actin filaments are assumed to act as a physical barrier that prevents the apical invasion of large organelles. Indeed, we found that the presence of correctly organized actin filaments is required to prevent apical invasion of large organelles (Figure 5).

Our observations suggest that cortical and internal apical actin filaments perform distinct functions in terms of the regulation of vesicle trafficking (Figures 3 and 4). Their combinatorial effect on vesicle trafficking is expected to lead to tip-directed vesicle transport and generation of the inverted “V” cone-shaped vesicle distribution (Figure 7A), which guarantees the delivery of materials necessary for pollen tube growth to the tip. Packaging of cortical apical actin filaments into linear bundles with uniform polarity, in which their barbed ends are assumed to be anchored on the apical membrane (Cheung et al., 2010; Liu et al., 2015), allow them to serve as tracks for the barbed end-directed myosin XIs (Lee and Liu, 2004). Consistent with our findings, a previous report showed that actin polymerization is necessary for the accumulation of secretory vesicles in the apical inverted cone (Lee et al., 2008). In addition, we demonstrate that actin filaments do exist within the core of the cytoplasm at the subapex and assume fine distribution supported by our measurement and modeling results (Figure 4C–4G). This differs from the notion that the subapical core of cytoplasm is devoid of actin filaments (Lovy-Wheeler et al., 2005), but it is consistent with the observations of actin filaments within the subapical region revealed by different actin markers in living pollen tubes (Cheung et al., 2008). Furthermore, our study demonstrates that internal apical actin filaments are involved in regulating the backward movement of vesicles, presumably by acting as a physical barrier. In support of our findings, a previous study showed that overexpression of RIC3, which depolymerizes apical actin filaments, leads to the even distribution of vesicles in the cytoplasm rather than the inverted cone distribution (Lee et al., 2008). The inhibitory effect of internal apical actin filaments on backward movement of vesicles may allow the tip-released vesicles to stay there for a while, thus permitting subsequent vesicle docking and fusion events. Our finding that cortical and internal apical actin filaments perform distinct functions in driving the transport and apical accumulation of vesicles is different

from the viewpoint that actin filaments within the growth domain act as the filter to allow apical invasion of small vesicles but prevent the entrance of large organelles into the apical region in the pollen tube (Kost et al., 1998; Cheung et al., 2008).

The active vesicle transport function of apical actin filaments was even more evident during the turning of pollen tubes. During turning, the whole apical actin structure reorients and guides the movement of vesicles toward the new tube growth direction (Figure 6). The reorientation of the apical actin structure toward the new tube growth direction is even more obvious in *rbohH* mutant pollen tubes, which undergo frequent turning (Supplemental Figure 7). Specifically, we found that apical actin filaments at the facing side undergo rapid depolymerization and repolymerization during tube turning, while polymerization and/or filament bundling is maintained or even upregulated at the opposite side (Figure 6). Actin filaments at the opposite side may take on the role of tip-directed vesicle transport, while apical actin filaments depolymerize on the facing side. Consequently, the dynamic reorganization of the apical actin structure allows the targeted delivery of vesicles to the new growth direction to guarantee successful turning (Figure 7B).

Thus, our observations suggest that the apical actin structure is well suited to the control of vesicle trafficking during rapid and directional pollen tube growth. Given that the elongation of tip-growing plant cells (e.g., root hairs, moss protonematal cells, and fungi hyphae) must be accompanied by the secretion of materials necessary for cell-wall synthesis and membrane expansion, our findings may have general implications for understanding the regulatory role of actin during tip growth. Determination of the unique characteristics of the organization and dynamics of the apical actin structure in different tip-growing cellular systems may allow us to understand how the apical actin structure functions within specific cellular contexts. Such comparisons will definitely facilitate the progress of investigations into the regulatory mechanisms underlying tip growth.

Arabidopsis Pollen Tube Serves as an Excellent Cellular System for Live-Cell Imaging

The pollen tube is an excellent cellular system for studying tip growth because it is easy to culture *in vitro* and, importantly, most of the features associated with pollen tubes grown *in vivo* are also observed *in vitro*. Historically, pollen tubes from tobacco and lily were used routinely because these species have large, easily germinated pollen grains, and it is therefore relatively easy to collect large amounts of pollen suitable

(G) Quantification of the position at which ARA7-positive endosomes reverse direction in *prf4 prf5* pollen tubes. A total of 263 motile endosomes were tracked in 18 pollen tubes.

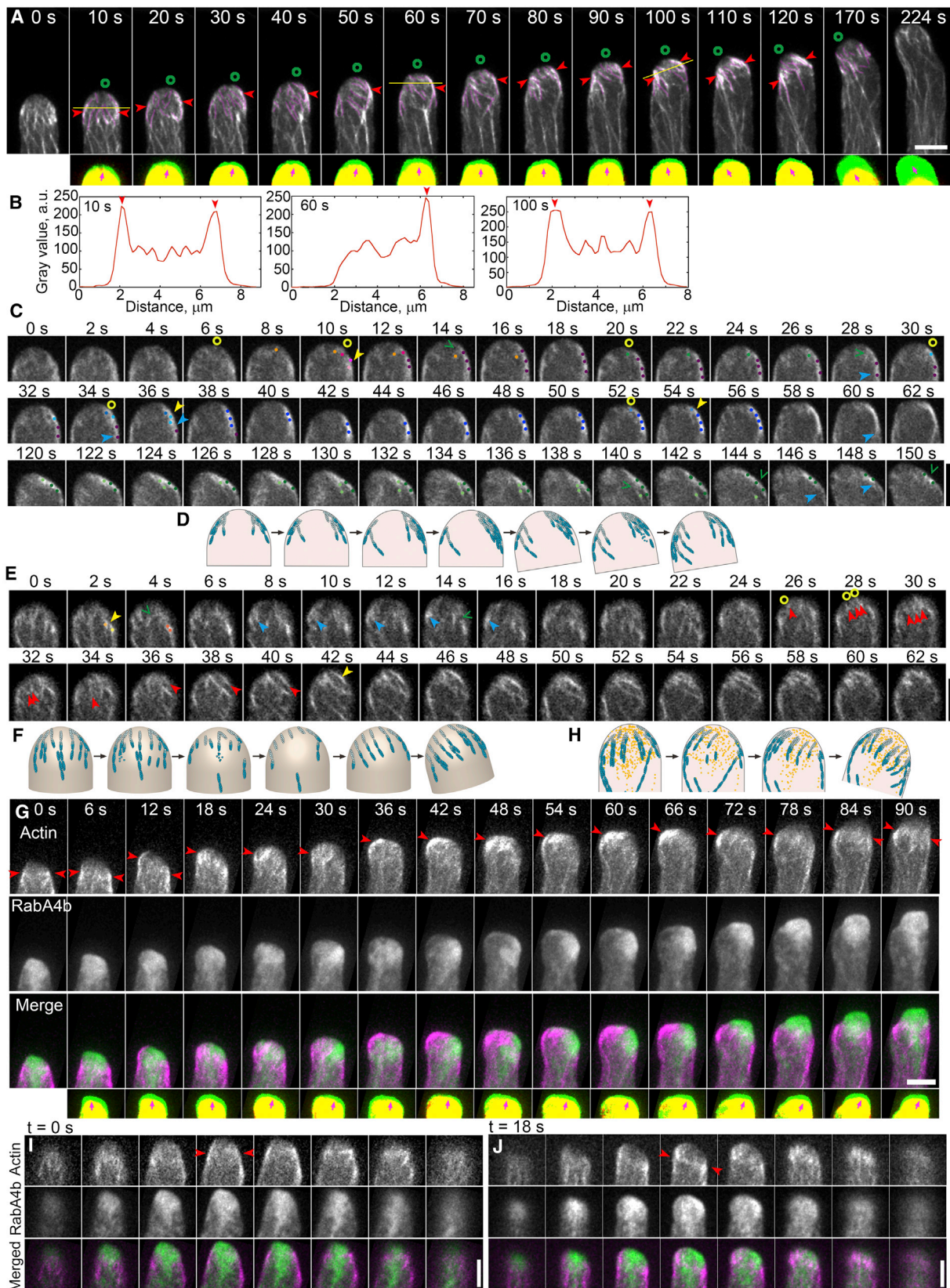
(H) Time-series images of a *vlm2 vln5* pollen tube harboring Lifeact-mCherry and YFP-ARA7. Red, yellow, and blue arrowheads indicate three individual endosomes that were tracked, and the white arrow indicates the position at which the vesicles reverse their direction of travel.

(I) Quantification of the location at which ARA7-positive endosomes reverse direction in *vlm2 vln5* pollen tubes. In total, 226 motile endosomes were tracked in 24 pollen tubes.

(J) Time-series images of a *fim5* pollen tube harboring ARA7-positive endosomes. Red arrowheads indicate a tracked individual vesicle.

(K) Quantification of the location at which ARA7-positive endosomes reverse direction in *fim5* pollen tubes. A total of 171 motile endosomes were tracked in 23 pollen tubes.

(L) Statistical comparison of the distance from the tip of the pollen tube at which ARA7-positive endosomes reverse their direction of travel in different genotypes. The average distance (mean \pm SD) is $4.64 \pm 1.26 \mu\text{m}$, $2.19 \pm 0.89 \mu\text{m}$, $2.25 \pm 1.31 \mu\text{m}$, and $2.26 \pm 1.11 \mu\text{m}$ in WT, *prf4 prf5*, *vlm2 vln5*, and *fim5* pollen tubes, respectively. ** $P < 0.01$ by Student's *t*-test, $n > 160$.



(legend on next page)

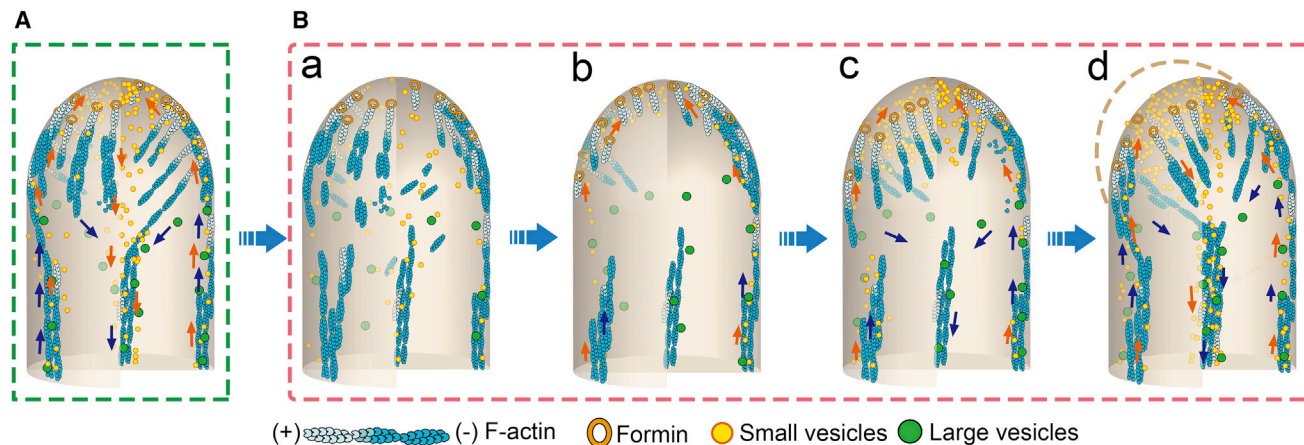


Figure 7. Schematic Depiction of the Relationship between Apical Actin Filaments and Vesicle Trafficking during Pollen Tube Growth and Turning.

Within a normal growing pollen tube (A), vesicles are transported directly to the tip along apical actin filaments at the cortex and released at the apical region centered at the polar axis. Internal apical actin filaments regulate the backward movement of vesicles from the tip, presumably by acting as a physical barrier. Meanwhile, apical actin filaments prevent the apical invasion of large organelles. During the turning of the pollen tube (B), apical actin filaments reorient toward the new tube growth direction. At the very beginning, most of the apical actin filaments depolymerize at the facing side but increase their bundling at the dorsal side (a). Subsequently, actin filaments will polymerize from the apical membrane at the facing side to facilitate the transport of vesicles toward the newly established expansion point of the pollen tube (b). Meanwhile, thick actin bundles at the dorsal side depolymerize to reorient the whole apical actin structure toward the new growth direction (c). The newly established apical actin structure will continuously transport materials toward the expanding domain of the pollen tube to ensure successful turning (d). Blue and red arrows indicate the direction of movement of large organelles and small vesicles, respectively. The orange dashed line indicates the new tube growth direction.

for microscopic observation. This study, along with several previous studies (Qu et al., 2013; Zhu et al., 2013; Qin et al., 2014; Liu et al., 2015; Zhou et al., 2015; Zhang et al., 2016a), has established the *Arabidopsis* pollen tube as an excellent system for live-cell imaging of the dynamics of actin filaments using spinning disk confocal microscopy. A major advantage of using *Arabidopsis* is that we can exploit the powerful functional genetics and genomic approaches that are available in this species. In this study, we showed that the overall organization, dynamics, and vesicle transport-based functions of apical actin filaments are conserved in pollen tubes from different

species, which suggests that the information gained from *Arabidopsis* regarding polarized cell growth can be applied to pollen tubes from other species. With the development of various live-cell imaging markers and advanced live-cell imaging technologies, such as spinning disk confocal microscopy, *Arabidopsis* pollen tubes would grow in popularity as a model for in-depth dissection of the cellular mechanisms underlying polarized cell growth.

In summary, we present new data with improved resolution and combining observations of the organization and dynamics of

Figure 6. Re-establishment of the Apical Actin Structure Precedes Morphological Change in a Turning Pollen Tube.

(A) Time-lapse images of actin filaments during the turning of a pollen tube. Green circles indicate the tube growth direction; red arrowheads indicate cortical apical actin filaments. In the lower panel, each image was created by merging two neighboring images from the upper panel. The green regions represent the new growth that has occurred between the two adjacent time points. Red arrowheads indicate the pollen tube growth direction.

(B) Quantification of the fluorescence intensity of actin filaments along the yellow lines in (A) that are perpendicular to the tube growth axis. Measurements were made at three different time points (10 s, 60 s, 100 s). The fluorescence peaks are indicated by red arrowheads.

(C) Time-lapse images of actin filaments in the medial section of a pollen tube during the turning process. Yellow circles indicate the newly polymerized actin filaments. Actin filaments marked by light purple, light blue, and light green dots undergo bundling to form the bundled actin filaments that are marked by dark purple, dark blue, and dark green dots, respectively. Filament bundling, depolymerization, and severing events are indicated by yellow, blue, and green arrowheads, respectively.

(D) Schematic depiction of actin filament dynamics in the inner region of the pollen tube during turning.

(E) Time-lapse images of actin filaments at the cortical region of a pollen tube during turning. Yellow circles indicated the newly polymerized actin filaments. Yellow, green, red, and blue arrowheads indicate filament bundling, severing, elongation, and depolymerization events, respectively.

(F) Schematic depiction of actin filament dynamics at the cortex of the pollen tube during turning.

(G) Simultaneous visualization of actin filaments (pink) and RabA4b-positive vesicles during tube turning. Red arrowheads indicate cortical apical actin filaments. The images in the small panels at the bottom were created by merging two neighboring images from the time series. The green regions represent the new growth that has occurred between two adjacent time points. Red arrows indicate the tube growth direction. See Supplemental Movie 6 for the entire series.

(H) Schematic model of the dynamics of actin filaments and vesicles during the turning of the pollen tube.

(I) z slices of the pollen tube shown in (G) at 0 s.

(J) z slices of the pollen tube shown in (G) at 18 s. Apical actin filaments reorient to guide the movement of vesicles toward the new growth direction, whereas no overt changes in tube morphology are detected. Red arrows in (I) and (J) indicate cortical apical actin filaments. Bars, 5 μm .

actin filament with vesicle transport within the growth domain of pollen tubes. This provides a more detailed and unified view regarding the overall organization and dynamics of apical actin filaments in pollen tubes. We demonstrate that the apical actin structure is well suited for the task of tip-directed transport and apical accumulation of vesicles that guarantees the rapidity of pollen tube growth.

METHODS

Pharmacological Treatments

Several inhibitors, including LatB, SMIFH2, and BDM, were used in this study to treat pollen tubes. These inhibitors were dissolved in DMSO to make stock solutions and were then added to liquid pollen germination medium (GM: 1 mM CaCl₂, 1 mM MgSO₄, 1 mM Ca(NO₃)₂, 0.01% H₃BO₃, 18% [w/v] sucrose, pH 7.0). Liquid GM containing the same concentration of DMSO was used as the control.

In Vitro Arabidopsis Pollen Germination

In vitro Arabidopsis pollen germination was performed as described previously (Ye et al., 2009; Zheng et al., 2013). Briefly, pollen derived from newly opened flowers was placed on GM (1 mM CaCl₂, 1 mM Ca(NO₃)₂, 1 mM MgSO₄, 0.01% [w/v] H₃BO₃, and 18% [w/v] sucrose solidified with 0.5% [w/v] agar, pH 7.0) and was cultured at 28°C under moist conditions.

Visualization of Actin Filaments, Endosomes, and Transport Vesicles in Living Pollen Tubes

The probes Lifeact-eGFP, YFP-RabA4b, and YFP-ARA7 were used to decorate actin filaments, transport vesicles, and endosomes, respectively, in *Arabidopsis* pollen tubes as described previously (Zhang et al., 2010b; Qu et al., 2013). These probes were introduced into mutants, including *fim5-1* (named as *fim5* in this paper) (Wu et al., 2010), *prf4 prf5* (Liu et al., 2015), and *vin2-1 vin5-2* (named as *vin2 vin5* in this paper) (Qu et al., 2013) by crossing the mutants with WT plants expressing these probes under the control of *Lat52*. Lifeact-eGFP was introduced into *rbohH* (Kaya et al., 2014) with the same strategy. To perform simultaneous visualization of actin filaments and endosomes or transport vesicles, Lifeact-mCherry was used as the probe to label actin filaments and was introduced into the mutant plants along with YFP-RabA4b or YFP-ARA7 by genetic crossing. F3 homozygous plants were used for the subsequent analysis. The segregating WT sibling plants harboring these probes were used as WT controls. To visualize the dynamics of actin filaments, endosomes, and transport vesicles in *Arabidopsis* pollen tubes, *Arabidopsis* pollen tubes were observed under a spinning disk confocal microscope equipped with a ×100 oil objective (1.4 numerical aperture). z stack time-series images were collected at 2 s intervals with the z step set at 0.5 μm with a Photometric Cascade II:512 EMCCD camera driven by Andor iQ2 software. The excitation wavelength was set at 488 nm, and the emission wavelength was set at 505–545 nm. To perform dual visualization of actin filaments and endosomes or transport vesicles in *Arabidopsis* pollen tubes, Lifeact-mCherry-decorated actin filaments were excited under a 563 nm argon laser, and YFP-RabA4b/YFP-ARA7-labeled vesicles were excited by a 488 nm argon laser. The images were subsequently processed and analyzed with ImageJ software (<http://rsbweb.nih.gov/ij/>; version 1.48g).

To determine the effect of LatB on the apical actin structure and the distribution of endosomes and transport vesicles, *Arabidopsis* pollen tubes expressing *Lat52::Lifeact-eGFP*, *Lat52::YFP-ARA7*, or *Lat52::YFP-RabA4b* were treated with 3 nM LatB. z stack time-series images were collected immediately after the application of LatB at 2 s intervals with the z step size set at 0.5 μm. To quantify the effect of LatB on the distribution of transport vesicles, the fluorescence pixel intensity of YFP-RabA4b was determined by measuring the gray value within the apical region with the

distance of its base about 5 μm away from the tip. At least 30 pollen tubes were measured. The distribution of YFP-ARA7-labeled endosomes was analyzed by measuring the coordinates of all YFP-ARA7-positive vesicles within 0–10 μm from the pollen tube tip, and 390 vesicles were finally selected. To observe the effect of BDM treatment on the distribution of RabA4b-positive transport vesicles, images were captured immediately after treatment with 10 mM BDM. Similarly, to assess the effect of BDM, we measured the gray values within a region with its base at a distance of about 5 μm from the pollen tube tip.

Visualization and Quantification of the Apical Actin Structure during Pollen Tube Growth

To simultaneously quantify the pollen tube growth rate and the fluorescence intensity of apical actin filaments, a kymograph was produced as previously described with slight modification (Liu et al., 2015). First, a 3-μm-wide line along the growth axis of the pollen tube was drawn, and the gray values along the line were measured using the ImageJ plugin StackProfileData (<http://rsb.info.nih.gov/ij/macros/StackProfileData.txt>). The text file was input into ImageJ to produce the kymograph. A threshold was set subsequently to distinguish the edge of the pollen tube, and the kymograph was converted to a mask. The background gray values were set to zero by multiplying the original images with the mask. Subsequent analyses were conducted on these modified kymographs. The real-time growth rate is measured by counting the movement of the position of the first non-zero gray value pixel. The real-time fluorescence intensity of apical actin filaments is measured by averaging the fluorescence intensity within the 5 μm region distal from the first non-zero gray value pixel. To visualize the change in fluorescence, the background pixel was cleared in Excel so that the tip of the pollen tube can be arranged in the same row. In order to enhance the contrast, the pseudo-color “Fire” was set by ImageJ.

Fluorescence Recovery after Photobleaching Assay

The FRAP assay was employed to assess the turnover rate of RabA4b-positive vesicles in *Arabidopsis* pollen tubes as described previously (Chang and Huang, 2015). To perform this experiment, two scan images were made as the pre-bleach contrast, and then a selected region about 10 μm away from the tip was bleached with the 458- and 488-nm laser lines at 100% transmission for 15 s. Time-lapse images were collected at 2 s intervals after photobleaching. Meanwhile, time-lapse images were collected from the unbleached region under the same image acquisition conditions and used to correct the bleaching effect during normal image collection. The average fluorescence pixel intensity of a region 0–5 μm from the tip was measured and plotted versus the elapsed time. Curve fitting was performed by ImageJ software with the following equation:

$$y = a \times (1 - \exp(-b \times x)) + c$$

where y is the fluorescence intensity, x is time, and a , b , c are the parameters of the curve.

Transient Gene Expression in Tobacco and Lily Pollen Tubes

To visualize the arrangement and dynamics of actin filaments in tobacco and lily pollen tubes, microparticle bombardment was employed according to previously published papers (Twell et al., 1989; Zhang et al., 2016b). The expression of *Lifeact-eGFP* in tobacco and lily pollen tubes was under the control of the promoters of *Lat52* and *Zm13*, respectively (Hamilton et al., 1992). To generate the pdGN-*Lat52::Lifeact-eGFP-nos* expression construct, a fragment containing *Lat52*, *Lifeact-eGFP*, and *NOS* terminator was amplified with primer pair *Lat52_{For}/NOS_{Rev}* (see Supplemental Table 1) using the plasmid pCambia 1301-*Lat52::Lifeact-eGFP-nos* (Qu et al., 2013) as the template, and the PCR products were moved into the pdGN vector (Lee et al., 2005) after digestion with *Sma*I/*Kpn*I to yield the final construct. To generate the pdGN-*Zm13::Lifeact-eGFP-nos* expression construct, the *Zm13* promoter was initially amplified with the primer pair *Zm13_{For}/Zm13_{Rev}* (see Supplemental

Table 1) using maize genomic DNA as the template. To replace *Lat52* with *Zm13*, *Zm13* was digested with *SmaI/SalI* then moved into *pdGN-Lat52::Lifeact-eGFP-nos*, which was cut with the same enzymes to generate *pdGN-Zm13::Lifeact-eGFP-nos*. Tobacco or lily pollen grains on a nitrocellulose membrane were bombarded three times by a PSD-1000/He particle delivery system (Bio-Rad), and 2.5 μ g of plasmid DNA were used each time. The bombarded pollen grains were germinated in GM and imaged with an Olympus BX61 microscope equipped with an Andor Revolution XDh spinning disk confocal system fitted with a \times 100 oil objective (1.4 numerical aperture). The excitation wavelength was 488 nm, and the emission wavelength was 505–545 nm.

SUPPLEMENTAL INFORMATION

Supplemental Information is available at *Molecular Plant Online*.

FUNDING

This work was supported by grants from the Ministry of Science and Technology of China (2013CB945100) and the National Natural Science Foundation of China (31671390 and 31471266). X.Q. was supported by post-doctoral fellowships from Tsinghua-Peking Joint Center for Life Sciences and the China Postdoctoral Science Foundation (grant no. 2015M571028).

AUTHOR CONTRIBUTIONS

S.H. conceived and designed the research; X.Q., R.Z., M.Z., and M.D. performed the research; X.Q., R.Z., M.Z., Y.X., and S.H. analyzed the data; S.H. wrote the paper with input from the co-authors.

ACKNOWLEDGMENTS

We thank Dave Kovar (University of Chicago) for providing us with SMIFH2 and Yan Zhang (Shandong Agricultural University) for the marker lines expressing YFP-RabA4b and YFP-ARA7 in pollen. We also thank Noni Franklin-Tong (University of Birmingham) for critical comments on revising this manuscript. No conflict of interest declared.

Received: February 3, 2017

Revised: April 15, 2017

Accepted: May 1, 2017

Published: May 10, 2017

REFERENCES

- Bloch, D., Pleskot, R., Pejchar, P., Potocky, M., Trpkosova, P., Cwiklik, L., Vukasinovic, N., Sternberg, H., Yalovsky, S., and Zarsky, V. (2016). Exocyst SEC3 and phosphoinositides define sites of exocytosis in pollen tube initiation and growth. *Plant Physiol.* **172**:980–1002.
- Bosch, M., Cheung, A.Y., and Hepler, P.K. (2005). Pectin methylesterase, a regulator of pollen tube growth. *Plant Physiol.* **138**:1334–1346.
- Bove, J., Vaillancourt, B., Kroeger, J., Hepler, P.K., Wiseman, P.W., and Geitmann, A. (2008). Magnitude and direction of vesicle dynamics in growing pollen tubes using spatiotemporal image correlation spectroscopy and fluorescence recovery after photobleaching. *Plant Physiol.* **147**:1646–1658.
- Brawley, C.M., and Rock, R.S. (2009). Unconventional myosin traffic in cells reveals a selective actin cytoskeleton. *Proc. Natl. Acad. Sci. USA* **106**:9685–9690.
- Chang, M., and Huang, S. (2015). *Arabidopsis* ACT11 modifies actin turnover to promote pollen germination and maintain the normal rate of tube growth. *Plant J.* **83**:515–527.
- Chen, C.Y., Wong, E.I., Vidali, L., Estavillo, A., Hepler, P.K., Wu, H.M., and Cheung, A.Y. (2002). The regulation of actin organization by actin-depolymerizing factor in elongating pollen tubes. *Plant Cell* **14**:2175–2190.
- Chen, N., Qu, X., Wu, Y., and Huang, S. (2009). Regulation of actin dynamics in pollen tubes: control of actin polymer level. *J. Integr. Plant Biol.* **51**:740–750.
- Cheung, A.Y., and Wu, H.M. (2007). Structural and functional compartmentalization in pollen tubes. *J. Exp. Bot.* **58**:75–82.
- Cheung, A.Y., and Wu, H.M. (2008). Structural and signaling networks for the polar cell growth machinery in pollen tubes. *Annu. Rev. Plant Biol.* **59**:547–572.
- Cheung, A.Y., Duan, Q.H., Costa, S.S., de Graaf, B.H., Di Stilio, V.S., Feijo, J., and Wu, H.M. (2008). The dynamic pollen tube cytoskeleton: live cell studies using actin-binding and microtubule-binding reporter proteins. *Mol. Plant* **1**:686–702.
- Cheung, A.Y., Niroomand, S., Zou, Y.J., and Wu, H.M. (2010). A transmembrane formin nucleates subapical actin assembly and controls tip-focused growth in pollen tubes. *Proc. Natl. Acad. Sci. USA* **107**:16390–16395.
- Cole, R.A., and Fowler, J.E. (2006). Polarized growth: maintaining focus on the tip. *Curr. Opin. Plant Biol.* **9**:579–588.
- de Graaf, B.H., Cheung, A.Y., Andreyeva, T., Lévassieur, K., Kieliszewski, M., and Wu, H.M. (2005). Rab11 GTPase-regulated membrane trafficking is crucial for tip-focused pollen tube growth in tobacco. *Plant Cell* **17**:2564–2579.
- de Win, A.H., Pierson, E.S., and Derksen, J. (1999). Rational analyses of organelle trajectories in tobacco pollen tubes reveal characteristics of the actomyosin cytoskeleton. *Biophys. J.* **76**:1648–1658.
- Derksen, J., Rutten, T., Lichtscheidl, I.K., Dewin, A.H.N., Pierson, E.S., and Rongen, G. (1995). Quantitative analysis of the distribution of organelles in tobacco pollen tubes: implications for exocytosis and endocytosis. *Protoplasma* **188**:267–276.
- Dong, H., Pei, W., and Ren, H. (2012). Actin fringe is correlated with tip growth velocity of pollen tubes. *Mol. Plant* **5**:1160–1162.
- Franklin-Tong, V.E. (1999). Signaling and the modulation of pollen tube growth. *Plant Cell* **11**:727–738.
- Fu, Y. (2015). The cytoskeleton in the pollen tube. *Curr. Opin. Plant Biol.* **28**:111–119.
- Fu, Y., Wu, G., and Yang, Z. (2001). Rop GTPase-dependent dynamics of tip-localized F-actin controls tip growth in pollen tubes. *J. Cell Biol.* **152**:1019–1032.
- Funaki, K., Nagata, A., Akimoto, Y., Shimada, K., Ito, K., and Yamamoto, K. (2004). The motility of *Chara corallina* myosin was inhibited reversibly by 2,3-butanedione monoxime (BDM). *Plant Cell Physiol.* **45**:1342–1345.
- Geitmann, A., and Emons, A.M. (2000). The cytoskeleton in plant and fungal cell tip growth. *J. Microsc.* **198**:218–245.
- Geitmann, A., Snowman, B.N., Emons, A.M., and Franklin-Tong, V.E. (2000). Alterations in the actin cytoskeleton of pollen tubes are induced by the self-incompatibility reaction in *Papaver rhoeas*. *Plant Cell* **12**:1239–1251.
- Gibbon, B.C., Kovar, D.R., and Staiger, C.J. (1999). Latrunculin B has different effects on pollen germination and tube growth. *Plant Cell* **11**:2349–2363.
- Gu, Y., Fu, Y., Dowd, P., Li, S., Vernoud, V., Gilroy, S., and Yang, Z. (2005). A Rho family GTPase controls actin dynamics and tip growth via two counteracting downstream pathways in pollen tubes. *J. Cell Biol.* **169**:127–138.
- Guan, Y., Guo, J., Li, H., and Yang, Z. (2013). Signaling in pollen tube growth: crosstalk, feedback, and missing links. *Mol. Plant* **6**:1053–1064.
- Hamilton, D.A., Roy, M., Rueda, J., Sindhu, R.K., Sanford, J., and Mascarenhas, J.P. (1992). Dissection of a pollen-specific promoter

- from maize by transient transformation assays. *Plant Mol. Biol.* **18**:211–218.
- Hepler, P.K., and Winship, L.J. (2015). The pollen tube clear zone: clues to the mechanism of polarized growth. *J. Integr. Plant Biol.* **57**:79–92.
- Hepler, P.K., Vidali, L., and Cheung, A.Y. (2001). Polarized cell growth in higher plants. *Annu. Rev. Cell Dev. Biol.* **17**:159–187.
- Higaki, T., Kutsuna, N., Okubo, E., Sano, T., and Hasezawa, S. (2006). Actin microfilaments regulate vacuolar structures and dynamics: dual observation of actin microfilaments and vacuolar membrane in living tobacco BY-2 Cells. *Plant Cell Physiol.* **47**:839–852.
- Holweg, C., Honsel, A., and Nick, P. (2003). A myosin inhibitor impairs auxin-induced cell division. *Protoplasma* **222**:193–204.
- Hormanseder, K., Obermeyer, G., and Foissner, I. (2005). Disturbance of endomembrane trafficking by brefeldin A and calyculin A reorganizes the actin cytoskeleton of *Lilium longiflorum* pollen tubes. *Protoplasma* **227**:25–36.
- Kaya, H., Nakajima, R., Iwano, M., Kanaoka, M.M., Kimura, S., Takeda, S., Kawarazaki, T., Senzaki, E., Hamamura, Y., Higashiyama, T., et al. (2014). Ca²⁺-activated reactive oxygen species production by *Arabidopsis* RbohH and RbohJ is essential for proper pollen tube tip growth. *Plant Cell* **26**:1069–1080.
- Kost, B., Spielhofer, P., and Chua, N.H. (1998). A GFP-mouse talin fusion protein labels plant actin filaments in vivo and visualizes the actin cytoskeleton in growing pollen tubes. *Plant J.* **16**:393–401.
- Kroeger, J.H., Daher, F.B., Grant, M., and Geitmann, A. (2009). Microfilament orientation constrains vesicle flow and spatial distribution in growing pollen tubes. *Biophys. J.* **97**:1822–1831.
- Lancelle, S.A., and Hepler, P.K. (1992). Ultrastructure of freeze-substituted pollen tubes of *Lilium longiflorum*. *Protoplasma* **167**:215–230.
- Lee, Y.R., and Liu, B. (2004). Cytoskeletal motors in *Arabidopsis*. Sixty-one kinesins and seventeen myosins. *Plant Physiol.* **136**:3877–3883.
- Lee, J.Y., Taoka, K., Yoo, B.C., Ben-Nissan, G., Kim, D.J., and Lucas, W.J. (2005). Plasmodesmal-associated protein kinase in tobacco and *Arabidopsis* recognizes a subset of non-cell-autonomous proteins. *Plant Cell* **17**:2817–2831.
- Lee, Y.J., Szumlanski, A., Nielsen, E., and Yang, Z. (2008). Rho-GTPase-dependent filamentous actin dynamics coordinate vesicle targeting and exocytosis during tip growth. *J. Cell Biol.* **181**:1155–1168.
- Li, S., Dong, H., Pei, W., Liu, C., Zhang, S., Sun, T., Xue, X., and Ren, H. (2017). LIFH1-mediated interaction between actin fringe and exocytic vesicles is involved in pollen tube tip growth. *New Phytol.* **214**:745–761.
- Liu, X., Qu, X., Jiang, Y., Chang, M., Zhang, R., Wu, Y., Fu, Y., and Huang, S. (2015). Profilin regulates apical actin polymerization to control polarized pollen tube growth. *Mol. Plant* **8**:1694–1709.
- Lovy-Wheeler, A., Wilsen, K.L., Baskin, T.I., and Hepler, P.K. (2005). Enhanced fixation reveals the apical cortical fringe of actin filaments as a consistent feature of the pollen tube. *Planta* **221**:95–104.
- Lovy-Wheeler, A., Cardenas, L., Kunkel, J.G., and Hepler, P.K. (2007). Differential organelle movement on the actin cytoskeleton in lily pollen tubes. *Cell Motil. Cytoskeleton* **64**:217–232.
- Luo, N., Yan, A., and Yang, Z. (2016). Measuring exocytosis rate using corrected fluorescence recovery after photoconversion. *Traffic* **17**:554–564.
- Nagy, S., Ricca, B.L., Norstrom, M.F., Courson, D.S., Brawley, C.M., Smithback, P.A., and Rock, R.S. (2008). A myosin motor that selects bundled actin for motility. *Proc. Natl. Acad. Sci. USA* **105**:9616–9620.
- Nebenfuhr, A., Gallagher, L.A., Dunahay, T.G., Frohlick, J.A., Mazurkiewicz, A.M., Meehl, J.B., and Staehelin, L.A. (1999). Stop-and-go movements of plant Golgi stacks are mediated by the actomyosin system. *Plant Physiol.* **121**:1127–1142.
- Parton, R.M., Fischer-Parton, S., Watahiki, M.K., and Trewavas, A.J. (2001). Dynamics of the apical vesicle accumulation and the rate of growth are related in individual pollen tubes. *J. Cell Sci.* **114**:2685–2695.
- Qin, T., Liu, X., Li, J., Sun, J., Song, L., and Mao, T. (2014). *Arabidopsis* microtubule-destabilizing protein 25 functions in pollen tube growth by severing actin filaments. *Plant Cell* **26**:325–339.
- Qin, Y., and Yang, Z.B.A. (2011). Rapid tip growth: Insights from pollen tubes. *Semin. Cell Dev. Biol.* **22**:816–824.
- Qu, X., Zhang, H., Xie, Y., Wang, J., Chen, N., and Huang, S. (2013). *Arabidopsis* villins promote actin turnover at pollen tube tips and facilitate the construction of actin collars. *Plant Cell* **25**:1803–1817.
- Qu, X., Jiang, Y., Chang, M., Liu, X., Zhang, R., and Huang, S. (2015). Organization and regulation of the actin cytoskeleton in the pollen tube. *Front. Plant Sci.* **5**:786.
- Ren, H., and Xiang, Y. (2007). The function of actin-binding proteins in pollen tube growth. *Protoplasma* **230**:171–182.
- Rizvi, S.A., Neidt, E.M., Cui, J., Feiger, Z., Skau, C.T., Gardel, M.L., Kozmin, S.A., and Kovar, D.R. (2009). Identification and characterization of a small molecule inhibitor of formin-mediated actin assembly. *Chem. Biol.* **16**:1158–1168.
- Rounds, C.M., and Bezanilla, M. (2013). Growth mechanisms in tip-growing plant cells. *Annu. Rev. Plant Biol.* **64**:243–265.
- Rounds, C.M., Hepler, P.K., and Winship, L.J. (2014). The apical actin fringe contributes to localized cell wall deposition and polarized growth in the lily pollen tube. *Plant Physiol.* **166**:139–151.
- Staiger, C.J., Poulter, N.S., Henty, J.L., Franklin-Tong, V.E., and Blanchoin, L. (2010). Regulation of actin dynamics by actin-binding proteins in pollen. *J. Exp. Bot.* **61**:1969–1986.
- Steer, M.W., and Steer, J.M. (1989). Tansley review No. 16-pollen-tube tip growth. *New Phytol.* **111**:323–358.
- Stephan, O., Cottier, S., Fahlen, S., Montes-Rodriguez, A., Sun, J., Eklund, D.M., Klahre, U., and Kost, B. (2014). RISAP is a TGN-associated RAC5 effector regulating membrane traffic during polar cell growth in tobacco. *Plant Cell* **26**:4426–4447.
- Su, H., Zhu, J., Cai, C., Pei, W., Wang, J., Dong, H., and Ren, H. (2012). FIMBRIN1 is involved in lily pollen tube growth by stabilizing the actin fringe. *Plant Cell* **24**:4539–4554.
- Tominaga, M., Yokota, E., Vidali, L., Sonobe, S., Hepler, P.K., and Shimmen, T. (2000). The role of plant villin in the organization of the actin cytoskeleton, cytoplasmic streaming and the architecture of the transvacuolar strand in root hair cells of *Hydrocharis*. *Planta* **210**:836–843.
- Twell, D., Klein, T.M., Fromm, M.E., and McCormick, S. (1989). Transient expression of chimeric genes delivered into pollen by microprojectile bombardment. *Plant Physiol.* **91**:1270–1274.
- Vidali, L., McKenna, S.T., and Hepler, P.K. (2001). Actin polymerization is essential for pollen tube growth. *Mol. Biol. Cell* **12**:2534–2545.
- Vidali, L., Rounds, C.M., Hepler, P.K., and Bezanilla, M. (2009). Lifeact-mEGFP reveals a dynamic apical F-actin network in tip growing plant cells. *PLoS One* **4**:e5744.
- Wang, H., Zhuang, X., Cai, Y., Cheung, A.Y., and Jiang, L. (2013). Apical F-actin-regulated exocytic targeting of NtPPME1 is essential for construction and rigidity of the pollen tube cell wall. *Plant J.* **76**:367–379.
- Wu, Y., Yan, J., Zhang, R., Qu, X., Ren, S., Chen, N., and Huang, S. (2010). *Arabidopsis* FIMBRIN5, an actin bundling factor, is required for pollen germination and pollen tube growth. *Plant Cell* **22**:3745–3763.

The Apical Actin Structure in Pollen Tubes

- Yang, Z.** (2008). Cell polarity signaling in *Arabidopsis*. *Annu. Rev. Cell Dev. Biol.* **24**:551–575.
- Ye, J., Zheng, Y., Yan, A., Chen, N., Wang, Z., Huang, S., and Yang, Z.** (2009). *Arabidopsis* Formin3 directs the formation of actin cables and polarized growth in pollen tubes. *Plant Cell* **21**:3868–3884.
- Zhang, H., Qu, X., Bao, C., Khurana, P., Wang, Q., Xie, Y., Zheng, Y., Chen, N., Blanchoin, L., Staiger, C.J., et al.** (2010a). *Arabidopsis* VILLIN5, an actin filament bundling and severing protein, is necessary for normal pollen tube growth. *Plant Cell* **22**:2749–2767.
- Zhang, M., Zhang, R., Qu, X., and Huang, S.** (2016a). *Arabidopsis* FIM5 decorates apical actin filaments and regulates their organization in the pollen tube. *J. Exp. Bot.* **67**:3407–3417.
- Zhang, R., Chang, M., Zhang, M., Wu, Y., Qu, X., and Huang, S.** (2016b). The structurally plastic CH2 domain is linked to distinct functions of fimbrins/plastins. *J. Biol. Chem.* **291**:17881–17896.

Molecular Plant

- Zhang, Y., He, J., Lee, D., and McCormick, S.** (2010b). Interdependence of endomembrane trafficking and actin dynamics during polarized growth of *Arabidopsis* pollen tubes. *Plant Physiol.* **152**:2200–2210.
- Zheng, Y., Xie, Y., Jiang, Y., Qu, X., and Huang, S.** (2013). *Arabidopsis* actin-depolymerizing factor7 severs actin filaments and regulates actin cable turnover to promote normal pollen tube growth. *Plant Cell* **25**:3405–3423.
- Zhou, Z., Shi, H., Chen, B., Zhang, R., Huang, S., and Fu, Y.** (2015). *Arabidopsis* RIC1 severs actin filaments at the apex to regulate pollen tube growth. *Plant Cell* **27**:1140–1161.
- Zhu, L., Zhang, Y., Kang, E., Xu, Q., Wang, M., Rui, Y., Liu, B., Yuan, M., and Fu, Y.** (2013). MAP18 regulates the direction of pollen tube growth in *Arabidopsis* by modulating F-actin organization. *Plant Cell* **25**:851–867.